Cheng, Harrison; Xie, Yao; Pellionisz, Peter; Pearigen, Aidan; Rangwalla, Khuzaima; Stafsudd, Oscar; Taylor, Zachary; St John, Maie; Grundfest, Warren

Dynamic optical contrast imaging (DOCI)

Published in:
Medical Imaging 2019

DOI:
10.1117/12.2513823

Published: 01/01/2019

Document Version
Publisher's PDF, also known as Version of record

Dynamic optical contrast imaging (DOCI): system theory for rapid, wide-field, multispectral optical imaging using fluorescence lifetime contrast mechanism

Harrison Cheng, Yao Xie, Peter Pellionisz, Aidan Pearigen, Khuzaima Rangwalla, et al.

Harrison Cheng, Yao Xie, Peter Pellionisz, Aidan Pearigen, Khuzaima Rangwalla, Oscar Stafsudd, Zachary Taylor, Maie St. John, Warren Grundfest, "Dynamic optical contrast imaging (DOCI): system theory for rapid, wide-field, multispectral optical imaging using fluorescence lifetime contrast mechanism," Proc. SPIE 10951, Medical Imaging 2019: Image-Guided Procedures, Robotic Interventions, and Modeling, 109512T (8 March 2019); doi: 10.1117/12.2513823

SPIE.

Event: SPIE Medical Imaging, 2019, San Diego, California, United States

Dynamic Optical Contrast Imaging (DOCI): System theory for rapid, wide-field, multispectral optical imaging using fluorescence lifetime contrast mechanism

Harrison Cheng[a], Yao Xie[b], Peter Pellionisz[a], Aidan Pearigen[a], Khuzaima Rangwalla[a], Oscar Stafsudd[b], Zachary Taylor[a,b,c], Maie St. John[a,d], and Warren Grundfest[a,b]

[a]Department of Bioengineering–UCLA, Henry Samueli School of Engineering and Applied Sciences, Los Angeles, USA
[b]Department of Electrical & Computer Engineering–UCLA, Henry Samueli School of Engineering and Applied Sciences, Los Angeles, USA
[c]Department of Electronics & Nanoengineering–Aalto University, Helsinki, Finland
[d]Department of Head & Neck Surgery–UCLA, David Geffen School of Medicine, Los Angeles, USA

ABSTRACT

Dynamic Optical Contrast Imaging (DOCI) is an imaging technique that generates image contrast through ratiometric measurements of the autofluorescence decay rates of aggregate fluorophores in tissue. This method enables better tissue characterization by utilizing wide-field signal integration, eliminating constraints of uniform illumination, and reducing time-intensive computations that are bottlenecks in the clinical translation of traditional fluorescence lifetime imaging. Previous works have demonstrated remarkable tissue contrast between tissue types in clinical human pilot studies. However, there are still challenges in the development of several subsystems, which results in existing works to use relative models. A comprehensive mathematical framework is presented to describe the contrast mechanism of the DOCI system to allow intraoperative quantitative imaging, which merits consideration for evaluation in measuring tissue characteristics in several important clinical settings.

Keywords: SPIE Proceedings, Dynamic Optical Contrast Imaging, Fluorescence Lifetime, System Theory, Real-time Imaging

1. INTRODUCTION

Dynamic optical contrast imaging (DOCI) is an imaging technique that seeks to generate contrast from relative differences in fluorophore lifetime ratios without the need to compute absolute lifetime values. Conventional fluorescence lifetime imaging microscopy (FLIM) is a powerful tool for tissue differentiation in the *ex vivo* lab setting, but complex, computationally intensive data fitting routines are impractical towards real-time visualization and intraoperative guidance for the surgeon. Data are often fit to an exponential decay model, a set of Laguerre polynomials, or frequency analysis from the phasor approach to extract coefficients related to decay times.[1–5] In addition, uniquely resolving the macroscopic lifetimes of heterogeneous tissues remains challenging when considering unknown mixing ratios, diverse multi-exponentials, and variations in individual fluorophore lifetimes due to underlying physiological and biochemical properties of tissue.[6]

The DOCI method is a ratiometric version of time-resolved autofluorescence imaging in which the weighted ratios of endogenous tissue fluorophore lifetimes provides image contrast.[7] These fluorophores mainly consist of collagen, elastin, reduced nicotinamide adenine dinucleotide (NADH), oxidised flavins, lipofuscin, keratin, and porphyrins.[8] Fluorescence lifetime is an intrinsic property of tissue that DOCI exploits in order to provide

Further author information: (Send correspondence to A.A.A.)
A.A.A.: E-mail: hcheng14@ucla.edu, Telephone: 1 206 788 7202
B.B.A.: E-mail: warrenbe@seas.ucla.edu, Telephone: 1 310 794 5550

Medical Imaging 2019: Image-Guided Procedures, Robotic Interventions, and Modeling, edited by Baowei Fei, Cristian A. Linte, Proc. of SPIE Vol. 10951, 109512T · © 2019 SPIE
CCC code: 1605-7422/19/$18 · doi: 10.1117/12.2513823

quantitative measurements via an image. Furthermore, the absence of dye or injected contrast simplifies use of the technique in an intraoperative environment. Prior work have provided a conceptual approach for the DOCI algorithm;[9–11] and remarkable contrast have been demonstrated between different tissue types in *ex vivo* pilot studies with human tissue.[12,13] The aim of this work is to mathematically model the DOCI system through rigorous proofs to describe the contrast mechanism of the system and differentiate DOCI from existing fluorescence lifetime imaging methodologies.

2. FLUORESCENCE LIFETIME OVERVIEW

A fluorophore excited by a photon may spontaneously emit another photon through the phenomenon of fluorescence. This process has been modeled as a first order differential equation and is shown in Eq. (1), where a is the rate of decay and $f(t)$ is the fluorescence intensity response with respect to time. Notably, this formula assumes the fluorophore does not possess multiple conformational states of different lifetimes.

$$\frac{df(t)}{dt} = -af(t) \tag{1}$$

When solving for the first order differential equation, the resultant time-domain response is an exponential decay as shown in Eq. (2) where i_0 is the initial fluorescence yield and τ is the inverse of the decay rate (a), termed the time it takes for the decay to reach 37% of the initial response.[8]

$$f(t) = i_0 e^{-at} = i_0 e^{\frac{-t}{\tau}} \tag{2}$$

Conventionally, the methods for acquiring fluorescence lifetime data operate in the time-domain or the frequency-domain. The optical setup and utilized detectors will differ in regards to the chosen technique. The measured response of the acquired fluorescence lifetime signal, however, $g(t)$ can be commonly described as the convolution of the fluorescence decay response $f(t)$ and the excitation response $h(t)$, as shown in Eq. (3).

$$g(t) = f(t) * h(t) \tag{3}$$

Figure 1 illustrates the excitation of a fluorophore with the subsequent fluorescence optical response in both the conventional time-domain and also the frequency-domain lifetime techniques.

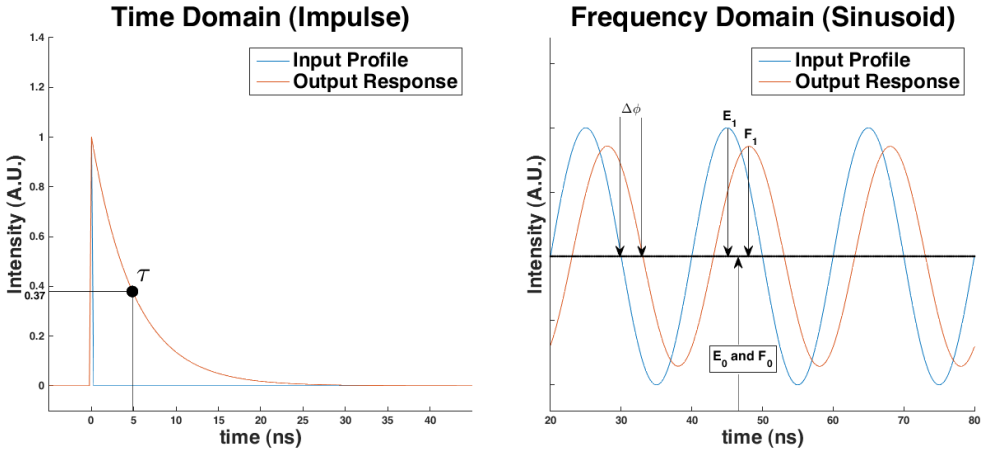

Figure 1. (left) Example of conventional time-domain method and (right) frequency domain method.

Following data acquisition, the fluorescence lifetime constant τ for both approaches is mathematically calculated. In the time-domain method, an ultra-short subnanosecond full-width half-maximum laser pulse is generally used as the source of excitation, which can be modeled as a dirac δ(t) function as $i(t)$.[14] Experimentally, the input source will typically exhibit a subnanosecond full-width half-maximum Gaussian pulse. This requires deconvolving the measured decay profile with the excitation pulse before performing the decay fit to accurately

extract mono-exponential fluorescence lifetime. Otherwise, if the deconvolution is not performed, the computed fluorescence decay would seem slightly longer than the actual lifetime property.[8]

The homodyne frequency-domain fluorescence lifetime method uses an excitation source that is modulated in a sinusoidal pattern. The fluorescence lifetime response can then be extracted using the amplitude *(M)*, phase *(ϕ)*, and frequency *(ω)* of the modulated excitation and resultant fluorescence response as shown in Eq. (4) and Eq. (5). Eq. (6) shows the magnitude ratio for amplitude based lifetime.

$$\tau_{\phi} = \frac{tan(\Delta\phi)}{\omega} \tag{4}$$

$$\tau_{Amp} = \frac{\sqrt{\frac{1}{M^2-1}}}{\omega} \tag{5}$$

$$M = \frac{F_1 E_0}{F_0 E_1} \tag{6}$$

Practical concerns when using these methods include: conventional time-domain methods are the long computation times (>1min/image) needed when trying to reconstruct high pixel count images;[15] and frequency-domain excitation also typically exhibit higher average power illumination that is not practical for biological samples.[16] Also, the different initial conditions and assumptions can result in decay constant profiles that are non-unique for multi-exponential decays. The DOCI method does not suffer from these disadvantages. Instead, the DOCI method was developed because it is impractical to uniquely identify all relevant fluorophores, know their mixing ratios, and pinpoint the dynamically changing lifetimes due to physiological effects. The trade-off of the DOCI method is to sacrifice identification of fluorophore for speed and practicality while offering enough contrast for tissue separation.

3. DOCI SYSTEM THEORY & MODEL

DOCI is a technique that seeks to generate contrast from relative differences in fluorophore lifetimes without the need to compute absolute lifetime values. This eliminates the complex, computationally intensive data fitting routines that has prevented successful translation of using fluorescence lifetime properties to differentiate tissue types. The mathematics behind the ideal system is to utilize relatively long pulse widths (>20 ns) with short fall times (∼1 ns) to produce contrast between fluorophores of different decay rates. Figure 2 shows how the DOCI method differs from conventional FLIM methods.

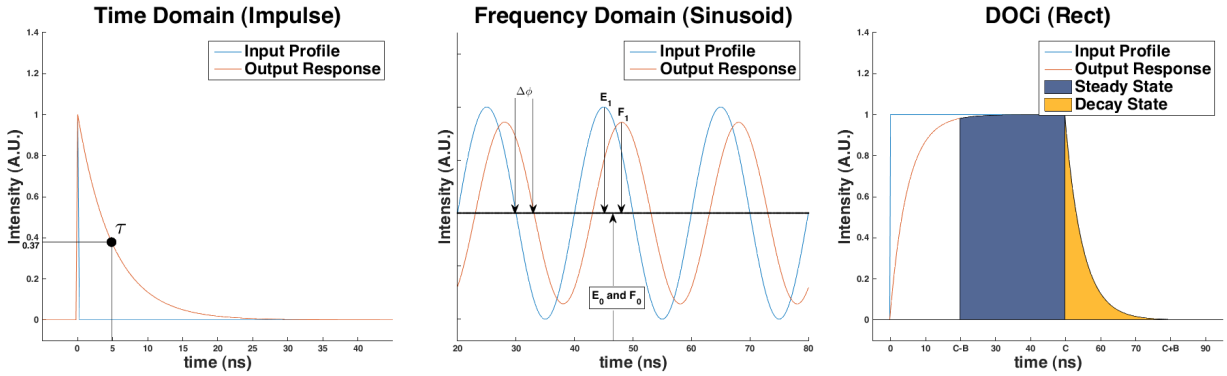

Figure 2. (left) Comparison between conventional time-domain method, (center) frequency domain method (center), and (right) DOCI method.

The DOCI system uses a rectangular illumination source and is modeled as a rectangular function. Unlike conventional FLIM methods where multiple data points at different time points are acquired, the DOCI method acquires two data points by integrating fluorescence signals at two specific time intervals - the steady state and the decay state. The steady state is used as a reference peak intensity for normalization and the decay state

represents fluorophores. Previous work have demonstrated the initial concept and promising human *ex vivo* pilot study image results have been demonstrated from the DOCI system.[17,18] Several mathematical expressions have been formulated to describe the behavior of the DOCI system and how the contrast mechanism is interpreted. Non-ideal models and assumptions are also provided when the illumination source contains a first-order decay because the illumination source cannot be experimentally turned off instantaneously.

3.1 Idealized Model

In the idealized model, the fluorophore is treated as first order differential equations while the illumination source is set to be an ideal rectangular function. Eq. (7) reiterates the time-domain response for the first order differential equation as an exponential decay in which *f(t)* is the decay response as a function of time. Variables a and A_0 will be used as intermediary variables to replace $\frac{1}{\tau}$ and i_0 respectively to simplify calculations.

$$f(t) = i_0 e^{\frac{-t}{\tau}} = A_0 e^{-at} \tag{7}$$

The DOCI rectangular excitation is modeled as the subtraction between a step function and a shifted step function as shown in Eq. (8), in which *h(t)* is the rectangular excitation pulse as a function of time and C is the rectangular pulse width.

$$h(t) = u(t) - u(t - C) \tag{8}$$

Eq. (9) and Eq. (10) is the Laplace transform for the exponential decay and the rectangular pulse function respectively.

$$\mathcal{L}[f(t)] = F(s) = i_0\left(\frac{1}{s+a}\right) \tag{9}$$

$$\mathcal{L}[h(t)] = H(s) = \frac{1}{s} - \frac{e^{-Cs}}{s} \tag{10}$$

These two equations will be the primary models to explain the DOCI system theory and how its contrast mechanism differentiates from the other methodologies.

3.1.1 Single Exponential Model

The general model of the DOCI system can be described as a finite integration of the convolution between the rectangular response and the hypothetical exponential sample decay as shown in Eq. (11).

$$q(t) = \int_0^t (f * h)(t)dt \tag{11}$$

In order to expand upon Eq. (11) and to not get confused with the convolution integral from the DOCI integral, the time-domain DOCI algorithm can be expanded into a double integral as shown in Eq. (12).

$$q(t) = \int_0^t \int_{-\infty}^{\infty} f(\tau)h(t-\tau)d\tau dt \tag{12}$$

Due to the complex nature of the equation in the time-domain, a closed form solution can be derived by defining the DOCI Laplace form *Q(s)* in Eq. (13) and calculating the Laplace form of the DOCI method as shown in Eq. (14).

$$\mathcal{L}\{q(t)\} = \mathcal{L}\left\{\int (f * h)(t)dt\right\} = Q(s) \tag{13}$$

$$Q(s) = \frac{F(s)\cdot H(s)}{s} = A_0\left[\frac{1 - e^{-Cs}}{s^2(s+a)}\right] \tag{14}$$

Similarly, the time-domain DOCI (*q(t)*) can be redefined as the inverse Laplace transform as shown in Eq. (15).

$$\mathcal{L}^{-1}\{Q(s)\} = \mathcal{L}^{-1}\left\{\frac{F(s)\cdot H(s)}{s}\right\} = q(t) \tag{15}$$

This allows the determination of the closed form time-domain DOCI that removes the previous double integral as in Eq. (16).

$$q(t) = \frac{A_0}{a^2}\left[e^{-at} - 1 + at - \left(e^{-a(t-C)} - 1 + a(t-C)\right)u(t-C)\right] \tag{16}$$

Figure 3 shows an example output of the computed model *q(t)* with a 5ns decay with a 50ns pulse width(C) excitation. The derived closed form solution is compared with a discrete convolution of between a rectangular function with an exponential decay with temporal increment of 0.25ns.

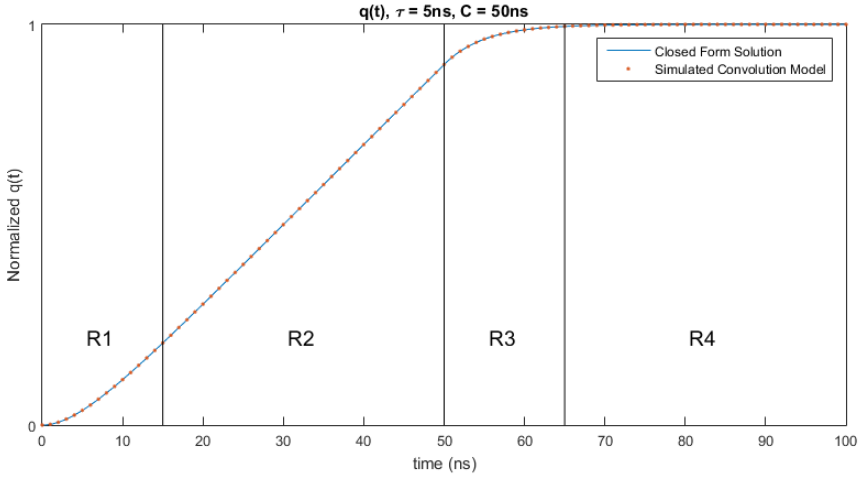

Figure 3. Comparison of the closed form solution and simulated convolution model for *q(t)*. The model is partitioned into four fluorescence states R1, R2, R3, and R4.

The two methods show identical results, which verifies the closed-form derivation. The model can be broken up into four distinct fluorescence states - R1, R2, R3, and R4, which corresponds to the fluorescence rise-time, steady state, decay state, and off-state respectively. The fluorescence steady-state and off-state can be approximated to be 3τ or 95% of the signal during the transient R1 and R3 regions respectively. However, this is not the complete DOCI method because the DOCI method integrates subregions of *q(t)* as previously shown in figure 2 and a division between the integral of the decay state by the integral of the steady state. Eq. (17) shows the complete form of the ideal DOCI method in which C is the pulse-width of the rectangular illumination source and B is the integration time.

$$DOCI = \frac{Decay\ State}{Steady\ State} = \frac{q(C+B) - q(C)}{q(C) - q(C-B)} \tag{17}$$

The region *q(C+B)* is the integral of the regions from *t=0* to *t=C+B* of *g(t)* as previously shown in figure 2. Likewise, the region *q(C)* is the integral of regions from *t=0* to *t=C*. The integral of the decay region remains when *q(C)* is subtracted from *q(C+B)*. The steady-state follows synonymous analogy, but happens before the decay state. Eq. (18) shows the expanded form of the DOCI method for a sample following a single exponential.

$$\frac{q(C+B) - q(C)}{q(C) - q(C-B)} = \frac{A_0\frac{1}{a^2}[1 + e^{-a(C+B)} - e^{-aB} - e^{-aC}]}{A_0\frac{1}{a^2}[e^{-aC} - e^{-a(C-B)} + aB]} \tag{18}$$

Two assumptions are made to simplify this expanded form of the DOCI equation. Eq. (19) and Eq. (20) shows that the pulse-width must be much longer than integration time and the integration time must be much longer than the longest lifetime to be obtained respectively.

$$C \gg B \tag{19}$$

$$B \gg \tau \tag{20}$$

In the approximation, the pulse-width *(C)* should be at least 3x longer than the integration time *(B)* and the integration time *(B)* should be at least 3x longer than the longest fluorophore lifetime *(τ)* of interest. A reasonable upper bound lifetime is assumed to be 10ns. The exponential terms from the expanded DOCI equation can be approximated to be 0 with these assumptions as shown in Eq. (21), Eq. (22), and Eq. (23).

$$e^{-\frac{C}{\tau}} \rightarrow e^{-\frac{3B}{\tau}} = e^{-\frac{9\tau}{\tau}} \approx 0 \tag{21}$$

$$e^{-\frac{B}{\tau}} \rightarrow e^{-\frac{3\tau}{\tau}} = 0.050 \approx 0 \tag{22}$$

$$e^{-\frac{C+B}{\tau}} \rightarrow e^{-\frac{4B}{\tau}} = e^{\frac{12\tau}{\tau}} \approx 0 \tag{23}$$

The exponential from Eq. (22) seems to be much greater than the rest of the other exponentials. However, due to possible system noise and fluctuations, 0.05 or 5% error margin seems to be a reasonable estimation. Eq. (24) provides the result simplified DOCI equation after all the exponential terms are approximated to be 0.

$$DOCI = \frac{A_0 \frac{1}{a^2}[1 + \cancelto{0}{e^{-a(C+B)}} - \cancelto{0}{e^{-aB}} - \cancelto{0}{e^{-aC}}]}{A_0 \frac{1}{a^2}[\cancelto{0}{e^{-aC}} - \cancelto{0}{e^{-a(C-B)}} + aB]} \approx \frac{A_0 \frac{1}{a^2}}{A_0 \frac{1}{a^2} aB} \tag{24}$$

Finally, a is converted back to $\frac{1}{\tau}$ to show the relationship of the DOCI equation with the fluorophore lifetime as shown in Eq. (25).

$$DOCI \approx \frac{\cancel{A_0 \frac{1}{a^2}}}{\cancel{A_0 \frac{1}{a^2}} aB} = \frac{1}{aB} = \frac{\tau}{B} \tag{25}$$

The extracted DOCI value is proportional to the lifetime with a scaling factor of inverse integration time. This mathematical derivation provides a generalized concept for the DOCI model applied to a single-exponential sample and validates previous related-works.[7,10,11] However, previous work did not provide the analysis of the derived assumptions, which is essential for accurate and reproducible results, especially from system-to-system variations and long lifetime fluorophores.

3.1.2 Multi-exponential Model

Next, the DOCI model is presented in the case of multiple fluorophores of unknown concentration with varying fluorescence lifetime $\tau_0, \tau_1, ...\tau_n$, which is relevant for heterogeneous samples such as biological tissues. To aggregate multi-exponentials into the DOCI model, the previous a_0 and A_0 is redefined to a_i and A_i respectively. Eq. (26) shows a summation of multiple exponentials with different decay and fluorescence intensity.

$$f(t) = A_0 e^{-a_0 t} + A_1 e^{-a_1 t} + ... + A_n e^{-a_n t} \tag{26}$$

The fluorescence intensity A_0 is dependent on several factors, including non-uniform illumination, quantity of present fluorophore, and respective fluorescence yield. A benefit of the DOCI method is that the division process enables normalization of these above mentioned non-uniformities. The illumination fluence is constant across all fluorophore constituents and can be divided out, as detailed below. The convolution theorem still applies, but the distributive property of convolution is applied to separate variables as shown in Eq. (27).

$$q(t) = \int_0^t (f_0 * h)(t)dt + \int_0^t (f_1 * h)(t)dt + ... + \int_0^t (f_n * h)(t)dt \tag{27}$$

Similar to the single exponential model, Laplace transform is used to calculate the closed form solutions for each element i individually as shown in Eq. (28).

$$\int_0^t (f_i * h)(t)dt = \frac{A_i}{a_i^2}\left[e^{-a_i t} - 1 + a_i t - \left(e^{-a_i(t-C)} - 1 + a_i(t-C)\right)u(t-C)\right] \tag{28}$$

Likewise, the DOCI method from Eq. (17) and the assumptions made in Eq. (21), Eq. (22), and Eq. (23) is applied to the summation of multiple convolution integrals. However, the terms have to be aggregated in the

numerator and denominator independently. Only after the aggregation can terms between the numerator and denominator be canceled out. To reiterate, this is due to the system acquisition of the data in which only 2 frames are acquired independently with the DOCI system - the steady state and the decay state. Eq. (29) shows the resultant closed form solutions of the DOCI method for multiple lifetime decays.

$$\frac{Decay\ State}{Steady\ State} = \frac{q(C+B)-q(C)}{q(C)-q(C-B)} \approx \frac{A_0\tau_0^2 + A_1\tau_1^2 + \cdots + A_n\tau_n^2}{B(A_0\tau_0 + A_1\tau_1 + \cdots + A_n\tau_n)} \tag{29}$$

Eq. (30) shows a condensed summation version of the multi-exponential DOCI method.

$$\frac{A_0\tau_0^2 + A_1\tau_1^2 + \cdots + A_n\tau_n^2}{B(A_0\tau_0 + A_1\tau_1 + \cdots + A_n\tau_n)} = \frac{\sum_{i=0}^{n} A_i\tau_i^2}{B\sum_{i=0}^{n} A_i\tau_i} \tag{30}$$

This equation details the contrast mechanism of the DOCI system. The contrast visible from the pixels of the produced image is derived from different fluorophore yields, lifetimes, and augmented ratios. Furthermore, to decouple the non-uniform illumination from the rest of the detected fluorescence intensity, as shown in Eq. (31), where $\gamma(x,y)$ is the illumination profile as a function of space.

$$A_i = \gamma(x,y)A_i' \tag{31}$$

Unlike the single exponential where A_i is completely divided out, there are ratios that consists of the fluorescence yield and the fluorophore counts. The illumination profile from Eq. (32) is divided out and thus the DOCI system is resilient to non-uniform illumination in the ideal model (without considering signal to noise (SNR) of the system).

$$DOCI = \frac{\sum_{i=0}^{n} \gamma(x,y)A_i'\tau_i^2}{B\sum_{i=0}^{n} \gamma(x,y)A_i'\tau_i} = \frac{\cancel{\gamma(x,y)}\sum_{i=0}^{n} A_i'\tau_i^2}{\cancel{\gamma(x,y)}B\sum_{i=0}^{n} A_i'\tau_i} = \frac{\sum_{i=0}^{n} A_i'\tau_i^2}{B\sum_{i=0}^{n} A_i'\tau_i} \tag{32}$$

Although lifetime data can be decoupled from the illumination non-uniformity of the system, regions of dimmer illumination will produce result with worse SNR than regions that are well illuminated.

3.2 Model with Illumination Decay

Experimentally, it is difficult to generate an ideal rectangular excitation function as illumination sources can never turn on and off instantaneously. Furthermore, the DOCI method to allow for rapid wide-field imaging utilizes light-emitting diodes (LED), which has a longer decay time relative to conventional pulsed laser sources. A DOCI model that factors in the illumination sources decay is proposed, where the source is also approximated to follow a first order differential equation decay similar to that of a simple mono-exponential fluorophore. The illumination source decay is modeled as shown in Eq. (33). Also similar to defining the constants in the fluorophore exponential, the variables in the decay from the excitation source such that the $\frac{1}{\tau_{exc}}$ is redefined to be d and that the $\gamma(x,y)$ from the multi-exponential non-uniform source is used to describe the maximum illumination intensity at a specific location in space. The intent is to demonstrate that the DOCI method is also insensitive to illumination profile heterogeneity so long as it is above a certain signal-to-noise threshold.

$$g(t) = \gamma(x,y)e^{\frac{-t}{\tau_{exc}}} = \gamma(x,y)e^{-dt} \tag{33}$$

Eq. (34) shows the Laplace transform of the LED decay, which is synonymous to a single lifetime decay.

$$\mathcal{L}[g(t)] = G(s) = \frac{\gamma(x,y)}{s+d} \tag{34}$$

Eq. (35) shows the LED illumination profile modeled as the convolution of the rectangular pulse. A model that better represent the empirical illumination pulse shape *h'(t)* is the ideal pulse shape *h(t)* convolved by the LED decay *g(t)*.

$$h'(t) = h(t) * g(t) \tag{35}$$

The fluorescence response over time is more precisely the convolution of the single exponential empirical illumination pulse shape *h'(t)* with the fluorophore sample *f(t)*. Eq. (36) describes the DOCI system with the LED decay factored with sample fluorescence response through the associative property of convolution.

$$q(t) = \int_0^t (f * h * g)(t)dt = \int_0^t (f * h')(t)dt = q(t) = \int_0^t \int_{-\infty}^{\infty} f(\tau)h'(t-\tau)d\tau dt \tag{36}$$

This resultant equation is similar to that of Eq. (11), described previously in the ideal DOCI model. The closed form solution of this equation will be derived in the following sections also for both single and multiple exponential responses. In the current iteration of the DOCI system, the illumination uses 375nm ultraviolet-A (UV-A) LEDs, so the illumination decay times *($\sim 4ns$)* are comparable to biologic fluorescence decays so this factor cannot be neglected.

3.2.1 Single Exponential Model

Similar to the ideal DOCI derivation, the Laplace form of the DOCI method can be redefined in Eq. (37), which is the multiplication of the sample fluorescence decay *F(s)*, the rectangular pulse function *H(s)*, and the illumination decay function *G(s)*. Both a and d are the inverse lifetime decays of the sample and illumination respectively.

$$\mathcal{L}[q(t)] = \frac{F(s) \cdot H(s) \cdot G(s)}{s} = \gamma(x,y)A_0' \left(\frac{1}{s^2(s+d)(s+a)} - \frac{e^{-Cs}}{s^2(s+d)(s+a)} \right) \tag{37}$$

The inverse Laplace transform from Eq. (37) is used to obtain the final time domain form of the 3-part convolution function shown in Eq. (38).

$$\begin{aligned} q(t) = \frac{\gamma(x,y)A_0'}{(d-a)} \Bigg(& \left[\frac{e^{-at} - 1 + at - \big(e^{-a(t-C)} - 1 + a(t-C)\big)u(t-C)}{a^2} \right] \\ & - \left[\frac{e^{-dt} - 1 + dt - \big(e^{-d(t-C)} - 1 + d(t-C)\big)u(t-C)}{d^2} \right] \Bigg) \end{aligned} \tag{38}$$

The constant $\frac{\gamma(x,y)A_0'}{(d-a)}$ is a function of the fluorescence yield, the illumination profile, and difference between the lifetime of the sample and the illumination decay. If the sample fluoresces longer than the time for the illumination to decay, the constant would be negative. At the same time, the subtraction between the two inverse squared terms will cancel out this negative constant. This is to demonstrate that the optical response *q(t)* should never be negative, regardless of the combinations of illumination decay or sample fluorescence. If the decay for both the sample and illumination is the same *(a=d)*, an equivalent alternative form is shown in Eq. (39) can be used.

$$q(t) = \tfrac{\gamma(x,y)A_0'}{d^3} \left(e^{-dt}(dt+2) - 2 + dt - \left[e^{-d(t-C)} \big(d(t-C)+2\big) sho - 2 + d(t-C) \right] u(t-C) \right) \tag{39}$$

Figure 4 shows the comparison of *q(t)* between the models with and without illumination decay.

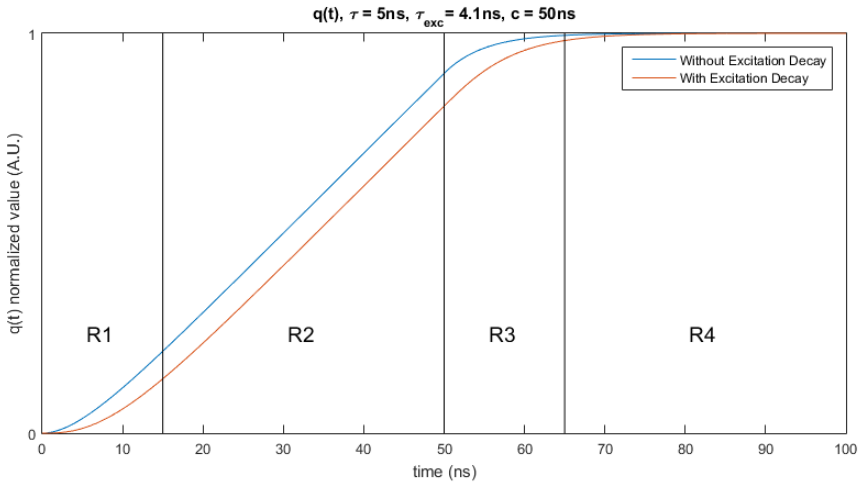

Figure 4. Comparison of *q(t)* between with and without excitation decay. The model is also partitioned into four fluorescence states R1, R2, R3, and R4.

The primary difference when illumination decay is factored in is that it takes slightly longer for the fluorescence profile to reach steady state and off state compared to a ideal rectangular excitation pulse. Eq. (40) shows the resultant expanded form when the DOCI method is applied.

$$\frac{Decay\ State}{Steady\ State} = \frac{\frac{\gamma(x,y)A_0'}{(d-a)}\left[\frac{1}{a^2}\left(1+e^{-a(C+B)}-e^{-aC}-e^{-aB}\right)-\frac{1}{d^2}\left(1+e^{-d(C+B)}-e^{-dC}-e^{-dB}\right)\right]}{\frac{\gamma(x,y)A_0'}{(d-a)}\left[\frac{1}{a^2}\left(e^{-aC}-e^{-a(C-B)}+aB\right]-\frac{1}{d^2}\left(e^{-dC}-e^{-d(C-B)}+dB\right)\right]} \tag{40}$$

The common constant $\frac{\gamma(x,y)A_0'}{(d-a)}$ can still be divided out, which reaffirms that the ideal DOCI method is insensitive to non-uniform illumination when signal-to-noise is not considered. However, a new fractional ratio terms of $\frac{1}{a^2}$, $\frac{1}{d^2}$ is introduced that was nonexistent in the previous models. This requires using the assumptions previously defined in Eq. (21), Eq. (22), and Eq. (23) to be qualified so that all the exponential terms can be approximated to be ∼0. Variable β is defined in Eq. (41) to be the summation of the dominant exponential terms and requires the DOCI system parameter selection so that the summation of these terms are less than or equal to 0.05 in order to approximate these terms to be 0.

$$\beta = \frac{e^{-aB}}{a^2} + \frac{e^{-dB}}{d^2} \leq 0.050 \approx 0 \tag{41}$$

These two terms are the dominant exponential terms that remains when selecting the DOCI system parameters as previously shown in Eq. (21), Eq. (22), and Eq. (23). The solution is to increase the integration time to be longer than the original 3τ. The length of the increase would depend on the decay of the illumination source and longest fluorophore lifetime of interest. This allows all of the exponential terms to be approximated as 0 and simplifies the DOCI model to be Eq. (42) after change of variables from a and d to $\frac{1}{\tau}$ and $\frac{1}{\tau_{exc}}$ respectively.

$$DOCI\ value = \frac{Decay\ State}{Steady\ State} \approx \frac{\cancel{\frac{\gamma(x,y)A_0'}{(\frac{1}{\tau_{exc}}-\frac{1}{\tau})}}(\tau^2-\tau_{exc}^2)}{\cancel{\frac{\gamma(x,y)A_0'}{(\frac{1}{\tau_{exc}}-\frac{1}{\tau})}}[B(\tau-\tau_{exc})]} = \frac{\tau+\tau_{exc}}{B} \tag{42}$$

When all terms are simplified, the DOCI value for the single exponential decay model is a function of the illumination decay time and the sample lifetimes divided by the integration time. The final equation simplifies down to a relatively intuitive model even with the double convolution that was introduced with the original mode. Figure 5 shows a simulated lifetime vs DOCI value of the derived linear model and the effects if β does not remain less than 0.05.

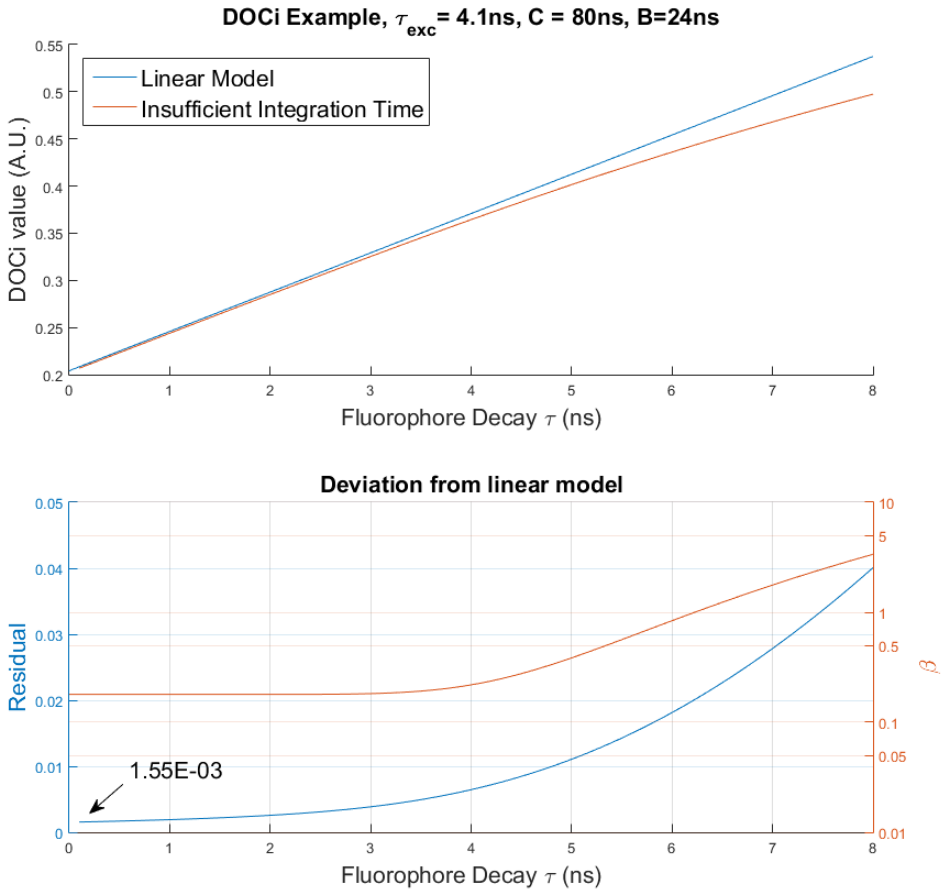

Figure 5. Simulated lifetime vs DOCI value of the derived linear model with elongated integration time.

Parameters that were used in the following example includes a 4.1ns illumination decay time, 80ns pulse-width and a 24ns integration time. Under these conditions, the residual error differences between the linear model and the derived model for lifetimes less than 5ns have ∼1% error. The β starts increasing exponentially after 5ns, which results in the deviation from the linear model to also start increasing exponentially. For a hypothetical 8ns fluorophore sample, which acts as upper bound for biological fluorophores, have errors approximate to be about ∼5% of the linear DOCI model. Although this error deviation on the order of ∼5% is relatively small, this error may be amplified when introducing other system-related noise. A solution to reduce this deviation would be to increase the integration time *(B)*, which will allow the error to be reduced to less than 1% as shown in figure 6.

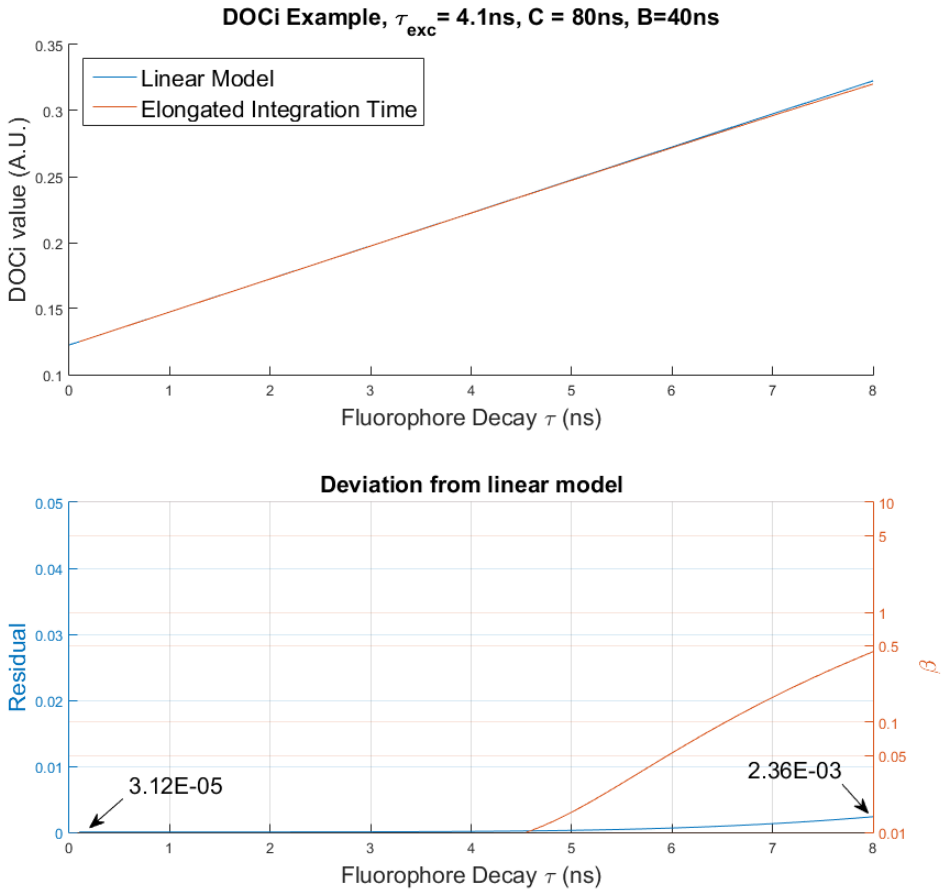

Figure 6. Simulated lifetime vs DOCI value of the derived linear model and the effects of β less than 0.05 on the derived model.

When the integration time is changed from 24ns to 40ns, the non-simplified model matches much more closely to the simplified linear model than the previous simulation. The residual is also 2 orders of magnitude less for short lifetime decays. At 8ns decay, deviation from the linear model occurs at <1%. In addition to better correlation with the intuitive linear model, increasing the integration time also maximizes the contrast between short and long lifetimes as well as potentially increasing signal-to-noise ratio. This single exponential model with illumination decay has similarity with its previous counterpart where $\gamma(x, y)$ can be divided out. This reaffirms that the DOCI value is independent of the illumination profile so long as SNR is high enough that noise is negligible. The terms $A'_0, A'_1, ...A'_n$ remain since they cannot be canceled out due to their ratio-like characteristics.

3.2.2 Multi-exponential Model

This section continues the derivation of the DOCI method with the illumination decay for multi-exponential fluorescence decays. From the previous section, Eq. (42) is derived to be the simplified form for single exponentials. For multi-exponentials, this equation can be generalized for each unique fluorophore as an index *(i)* as shown in Eq. (43).

$$\frac{Decay\ State_i}{Steady\ State_i} \approx \frac{\frac{\gamma(x,y)A'_i}{(\frac{1}{\tau_{exc}}-\frac{1}{\tau_i})}(\tau_i^2-\tau_{exc}^2)}{\frac{\gamma(x,y)A'_i}{(\frac{1}{\tau_{exc}}-\frac{1}{\tau_i})}[B(\tau_i-\tau_{exc})]} = \frac{\gamma(x,y)A'_i\tau_i\tau_{exc}(\tau_i+\tau_{exc})}{B\gamma(x,y)A'_i\tau_i\tau_{exc}} \tag{43}$$

This generalized form of the equation prior to division between the numerator and the denominator can then be expressed into a summation form for multi-exponential decays as shown in Eq. (44).

$$\frac{Decay\ State}{Steady\ State} \approx \frac{\sum_{i=0}^{n} \cancel{\gamma(x,y)} A_i' \tau_i \cancel{\tau_{exc}} (\tau_i + \tau_{exc})}{B \sum_{i=0}^{n} \cancel{\gamma(x,y)} A_i' \tau_i \cancel{\tau_{exc}}} = \frac{\sum_{i=0}^{n} A_i' \tau_i (\tau_i + \tau_{exc})}{B \sum_{i=0}^{n} A_i' \tau_i} \tag{44}$$

The illumination profile $\gamma(x, y)$ and τ_{exc} are common terms across all of the summed exponentials, which allows it to be simplified from the entire summation term. This final term is very similar to Eq. (30) that was previously derived for the ideal multi-exponential model, but with one of the τ_i term being replaced by $\tau_i + \tau_{exc}$.

Empirically, the illumination source used exhibits a 4-5ns decay, which is substantial considering that biological fluorophores under investigation have lifetimes between 1-10ns. Under conditions where the sample lifetime is much greater than the illumination decay time *(e.g* $\tau_i \gg \tau_{exc}$*)*, then the τ_{exc} can be assumed *0* and would reduce the equation back down to the ideal multi-exponential case. This final ratio equation permits a quantitative interpretation of the contrast mechanism given that certain assumptions hold. Initial pilot study's goal was to be able to identify different tissue types through relative DOCI value. However, as multiple systems systems were developed where each system were slightly different, a more robust and quantitative approach is needed to enable cross-platform data amalgamation and system standardization.

3.3 System Noise

Brief explanation of the system noise can be incorporated into the ideal model as this is still a work in progress. The decay state and the steady state signal that are acquired from the DOCI system are termed $Signal_{DS}$ and $Signal_{SS}$, respectively. The two signals that are acquired from the DOCI system are a composition of the true fluorescence signal and the background signal as shown in Eq. (45). To extract the true fluorescence signal, the background signal must be subtracted out before applying the division, as shown in Eq. (46).

$$\frac{Signal_{DS}}{Signal_{SS}} = \frac{Decay\ State + BG}{Steady\ State + BG} \tag{45}$$

$$\frac{Decay\ State}{Steady\ State} = \frac{Signal_{DS} - BG}{Signal_{SS} - BG} \tag{46}$$

Sources of noise in the DOCI system that can be empirically measured includes the detector background noise and the illumination flux. The noises sources are assumed to be Poisson distributed. Additionally, the DOCI method allows for >5KHz data acquisition rate, so as the sample size approach large values, the Poisson distribution can be approximate to follow a normal distribution. In a well-controlled in-vitro lab environment, the illumination flux per unit area can be accurately measured. However, this becomes difficult to reproduce in a clinical environment where there is high variations in imaging focal distances and object contours. There are also sources of noise from the sample because of its biochemical heterogeneity, dynamic chemical states (e.g. temperature, pH, oxygenation, hydration, etc..), and intermolecular interactions (quenching, bleaching, etc...). These are more difficult, if not impossible to measure or identify in fresh tissue because the physiologic dynamics prohibit repeatability. These measurements are also not clinically relevant as the goal is to identify the average signal distribution of tissue A from tissue B. Eq. (47) shows a model for the noise distribution.

$$\frac{Signal_{DS} - BG}{Signal_{SS} - BG} \sim \frac{\mathcal{N}(\mu_{Signal_{DS}}, \sigma_{Signal_{DS}}) - \mathcal{N}(\mu_{BG}, \sigma_{BG})}{\mathcal{N}(\mu_{Signal_{SS}}, \sigma_{Signal_{SS}}) - \mathcal{N}(\mu_{BG}, \sigma_{BG})} = \frac{\mu_{DS} \pm \sigma_{DS}}{\mu_{SS} \pm \sigma_{SS}} \tag{47}$$

By propagation of uncertainty, the signal distribution of the decay state and steady state can be approximated separately as shown in shown in Eq. (48) and Eq. (49) respectively.

$$\mu_{DS} \pm \sigma_{DS}^2 = \mu_{Signal_{DS}} - \mu_{BG} \pm \sigma_{Signal_{DS}}^2 + \sigma_{BG}^2 + 2cov(DS, BG) \tag{48}$$

$$\mu_{SS} \pm \sigma_{SS}^2 = \mu_{Signal_{SS}} - \mu_{BG} \pm \sigma_{Signal_{SS}}^2 + \sigma_{BG}^2 + 2cov(SS, BG) \tag{49}$$

When the two distributions are divided together, the DOCI signal distribution can be approximate as shown in Eq. (50).

$$DOCI = \frac{\mu_{DS} \pm \sigma_{DS}^2}{\mu_{SS} \pm \sigma_{SS}^2} = \frac{\mu_{DS}}{\mu_{SS}} \pm \frac{\sigma_{DS}}{\mu_{DS}}^2 + \frac{\sigma_{SS}}{\mu_{SS}}^2 - 2\frac{cov(DS, SS)}{\mu_{DS}\mu_{SS}} \tag{50}$$

The final form of the DOCI signal-to-noise distribution contains multiples ratio occurrences of the standard deviation from the steady state signal, decay state signal, and background. This equation can also be applied pixel to each pixel independently due to the method's insensitivity to illumination non-uniformity. Maximizing the signal or minimizing system noise has direct impact to the resolvable lifetime resolution.

3.4 Experimental Validation

Preliminary measurements with fluorescein dye samples were performed to validate the mathematical derivation for single exponential lifetime decay medium. In literature, fluorescein is cited to have ∼4ns fluorescence decay.[19,20] Conventional time-domain lifetime technique was first performed through curve fitting to extract the lifetime of the dye samples. This is done by acquiring 5 laser pulse measurements and 5 dye measurements. By using all 25 permutations of pulse-dye combinations, the results for fluorescein is 4.164±0.165ns, which agrees with literature values. After acquiring data using the conventional time-domain method, measurements using the DOCI method was acquired using the fluorescein sample. Figure 7 shows the empirical DOCI illumination decay profile and the respective fitted decay to identify the excitation illumination decay time (τ_{exc}).

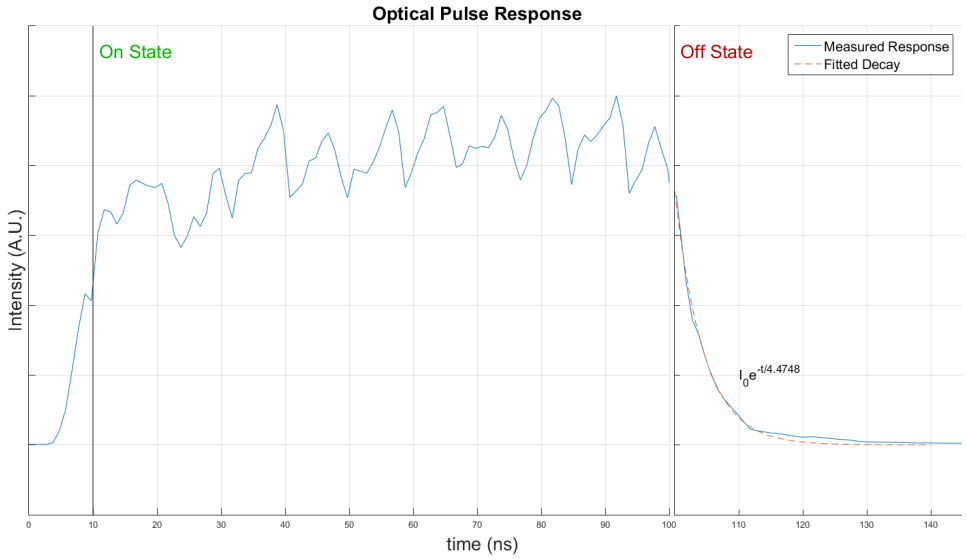

Figure 7. Extraction of illumination decay.

The fitted decay curve shows the illumination exhibiting a ∼4.48ns illumination decay. One concern is the oscillations that is seen in the steady state, which is due to impedance mismatch in the diode driver circuit and is currently a work in progress. However, these oscillations are relatively periodic and the peaks and troughs can potentially cancel each other out, with some offset in the steady state signal. Eq. (51) shows the derived single exponential model with illumination decay equation with the DOCI integration time *(B)* set to 40ns for this particular fluorescein (∼4.1ns) experiment. Based off these measurements the DOCI values can be hypothesized be ∼0.216±0.0041.

$$DOCI = \frac{\tau_{fluorescein} + \tau_{exc}}{B} = \frac{4.16 \pm 0.165ns + 4.48ns}{40ns} \approx [0.2119, 0.2201] \tag{51}$$

The DOCI method results in a unitless value after unit arithmetic. Figure 8 shows a histogram of the fluorescein DOCI value distribution obtained using the DOCI method.

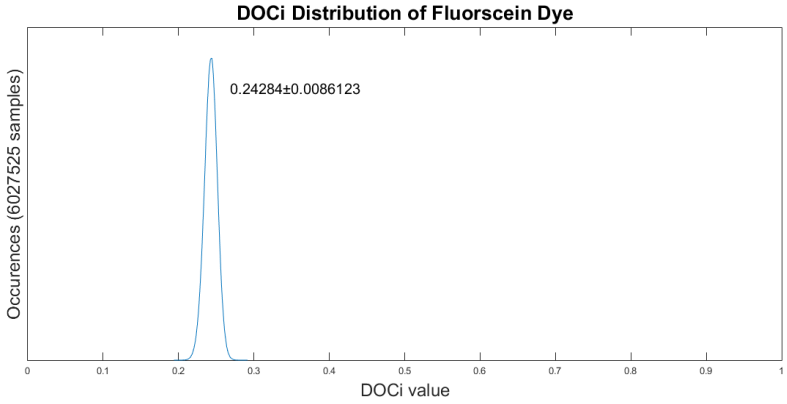

Figure 8. Histogram of fluorescein distribution using DOCI method.

Preliminary dye measurements was obtained by taking 5 sets of background images and 5 sets of fluorescein DOCI images using a 1Mpx scientific CCD to allow 25 unique permutations of the background-DOCI dataset. After performing image arithmetic from Eq. (46), a central subregion of interest from the final DOCI images were selected from each of the 25 datasets and aggregated to allow a >6million sample size. The minor deviation offset of 0.03 or ∼15% of the mean is attributable to the impedance mismatch oscillations in the illumination source circuit driver, slight inaccuracy in the timing of the integration states ± 2ns, or other sources of noise.

Results from this preliminary dye measurement reinforce the validity of DOCI theory with empirical evidence, with relatively minor imprecisions. A larger spread of dye samples will be further explored with detailed experimental setup and analysis procedure.

4. DISCUSSION

A single system was prototyped to demonstrate algorithm feasibility and clinical translatability in previous works. However, there are several challenges that exist in the development of the DOCI system such as creating a stable illumination source and system noise characterization. The primary limitation that results from these challenges is that the work reported to date use a relative system-specific models for device performances and data interpretation. This makes it difficult for massive data accumulation across heterogeneous tissues with many physiological confounding variables using multiple systems.

The derivation of the closed-loop model under different system and operating conditions allows for greater understanding of the effects of different subsystem variables on the DOCI data such as the illumination decay and system noise. This rigorous mathematical derivation is allows for quantitative imaging as oppose to relative system-specific imaging. More focused simulations and models can be independently developed for system characterization and improvement in data accuracy.

Although there are challenges in the device technology, specifically the illumination; the developed model will allow for better understanding on how these variations will affect the final data, and potentially allow for data aggregation across multiple systems. The preliminary results with fluorescein dye supports the utility of this system towards ratio-metric quantitative imaging in which a physical property can be correlated to a specific DOCI value. Although the errors are still relatively high, this still demonstrates that the results can be hypothesized and predicted based on quantitative measurements.

5. CONCLUSION

DOCI generates image contrast through relative measurements of the autofluorescence decay rates *(lifetime)* of aggregate fluorophores in tissue. The mechanism of this tool is non-invasive and does not require special dye or injection of exogenous contrast agents. This technique quantifies measurements of intrinsic fluorescence lifetime ratios unique to tissue types and permits display of additional information that is not available to the unaided

eye. It is superior to other fluorescence measuring approaches because the computation of absolute lifetime values is not required in this approach.

The simplicity of the data processing permits high-speed visualization of regions of interest suitable for translation into the clinic or the operating room. The presented derivation and results support ongoing efforts of adapting the algorithm to provide a useful tool for real-time intraoperative guidance. This novel tool warrants further investigation through large-scale clinical trial and engineering development in order to successfully expand the armamentarium of medical devices available to the physician.

ACKNOWLEDGMENTS

National Institute of Health (NIH) (1R01CA205051-01A1, 1R01CA220663-01A1); Tobacco-Related Disease Research Program of the University of California (TRDRP-UC) (24RT-0029); UCLA Medical Scientist Training Program (UCLA-MSTP) (T32GM008042). Kirby Vosburgh for external guidance and review of manuscript.

REFERENCES

[1] Kuwana, E. and Sevick-Muraca, E. M., "Fluorescence lifetime spectroscopy in multiply scattering media with dyes exhibiting multiexponential decay kinetics," *Biophysical Journal* **83**(2), 1165–1176 (2002).

[2] Jameson, D. M., Gratton, E., and Hall, R. D., "The measurement and analysis of heterogeneous emissions by multifrequency phase and modulation fluorometry," *Applied Spectroscopy Reviews* **20**(1), 55–106 (1984).

[3] Liu, H., Carpenter, C. M., Jiang, H., Pratx, G., Sun, C., Buchin, M. P., Gambhir, S. S., Xing, L., and Cheng, Z., "Intraoperative Imaging of Tumors Using Cerenkov Luminescence Endoscopy: A Feasibility Experimental Study," *Journal of Nuclear Medicine* **53**, 1579–1584 (10 2012).

[4] Digman, M. A., Caiolfa, V. R., Zamai, M., and Gratton, E., "The phasor approach to fluorescence lifetime imaging analysis," *Biophysical Journal* **94**(2), 14–16 (2008).

[5] Elder, A. D., Matthews, S. M., Swartling, J., Yunus, K., Frank, J. H., Brennan, C. M., Fisher, A. C., and Kaminski, C. F., "Application of frequency-domain Fluorescence Lifetime Imaging Microscopy as a quantitative analytical tool for microfluidic devices.," *Optics express* **14**(12), 5456–5467 (2006).

[6] Marcu, L., "Fluorescence lifetime techniques in medical applications," *Ann. Biomed. Eng. 40(2), 304331 (2012).* **40**(2), 304–331 (2012).

[7] Jiang, P.-C., Grundfest, W. S., and Stafsudd, O. M., "Quasi-real-time fluorescence imaging with lifetime dependent contrast," *Journal of Biomedical Optics* **16**(8), 086001 (2011).

[8] Berezin, M. Y. and Achilefu, S., "Fluorescence Lifetime Measurements and Biological Imaging," *Chem. Rev.* **110**(5), 2641–2684 (2010).

[9] Jiang, P.-C., Grundfest, W. S., and Stafsudd, O. M., "Quasi-real-time fluorescence imaging with lifetime dependent contrast," *Journal of Biomedical Optics* **16**(8), 086001 (2011).

[10] Papour, A., Taylor, Z., Sherman, A., Sanchez, D., Lucey, G., Liau, L., Stafsudd, O., Yong, W., and Grundfest, W., "Optical imaging for brain tissue characterization using relative fluorescence lifetime imaging.," *Journal of biomedical optics* **18**(6), 60504 (2013).

[11] Papour, A., Taylor, Z., Stafsudd, O., Tsui, I., and Grundfest, W., "Imaging autofluorescence temporal signatures of the human ocular fundus in vivo," *Journal of Biomedical Optics* **20**(11), 110505 (2015).

[12] Taylor, Z., Kim, I., Pesce, J., Grundfest, W., and St. John, M., "Dynamic Optical Contrast Imaging as a Novel Modality to Rapidly Distinguish Oral Squamous Cell Carcinoma From Surrounding Normal Tissue," *International Journal of Radiation Oncology*Biology*Physics* **94**(4), 921 (2016).

[13] Kim, I. A., Taylor, Z. D., Cheng, H., Sebastian, C., Maccabi, A., Garritano, J., Tajudeen, B., Razfar, A., Palma Diaz, F., Yeh, M., Stafsudd, O., Grundfest, W., and St. John, M., "Dynamic Optical Contrast Imaging: A Technique to Differentiate Parathyroid Tissue from Surrounding Tissues," *Otolaryngology-Head and Neck Surgery* **156**(3), 480–483 (2017).

[14] Boens, N., Qin, W., Basarić, N., Hofkens, J., Ameloot, M., Pouget, J., Lefèvre, J. P., Valeur, B., Gratton, E., VandeVen, M., Silva, N. D., Engelborghs, Y., Willaert, K., Sillen, A., Rumbles, G., Phillips, D., Visser, A. J. W. G., Van Hoek, A., Lakowicz, J. R., Malak, H., Gryczynski, I., Szabo, A. G., Krajcarski, D. T., Tamai, N., and Miura, A., "Fluorescence lifetime standards for time and frequency domain fluorescence spectroscopy," *Analytical Chemistry* **79**(5), 2137–2149 (2007).

[15] Keereweer, S., Van Driel, P. B. A. A., Snoeks, T. J. A., Kerrebijn, J. D. F., Baatenburg de Jong, R. J., Vahrmeijer, A. L., Sterenborg, H. J. C. M., and Löwik, C. W. G. M., "Optical image-guided cancer surgery: challenges and limitations.," *Clinical cancer research : an official journal of the American Association for Cancer Research* **19**(14), 3745–54 (2013).

[16] Roudot, P., Kervrann, C., and Waharte, F., "Lifetime estimation of moving vesicles in frequency-domain fluorescence lifetime imaging microscopy," *Proceedings - International Symposium on Biomedical Imaging* **32**(10), 668–671 (2012).

[17] Kim, I. A., Taylor, Z. D., Cheng, H., Sebastian, C., Maccabi, A., Garritano, J., Tajudeen, B., Razfar, A., Palma Diaz, F., Yeh, M., Stafsudd, O., Grundfest, W., and St. John, M., "Dynamic Optical Contrast Imaging: A Technique to Differentiate Parathyroid Tissue from Surrounding Tissues," *Otolaryngology-Head and Neck Surgery* **156**, 480–483 (3 2017).

[18] Tajudeen, B. A., Taylor, Z. D., Garritano, J., Cheng, H., Pearigen, A., Sherman, A. J., Palma-Diaz, F., Mishra, P., Bhargava, S., Pesce, J., Kim, I., Sebastian, C., Razfar, A., Papour, A., Stafsudd, O., Grundfest, W., and St. John, M., "Dynamic optical contrast imaging as a novel modality for rapidly distinguishing head and neck squamous cell carcinoma from surrounding normal tissue," *Cancer* **123**(5), 879–886 (2017).

[19] Magde, D., Rojas, G. E., and Seybold, P. G., "Solvent dependence of the fluorescence lifetimes of xanthene dyes," *Photochemistry and Photobiology* (1999).

[20] Elmgren, H., "The fluorescence lifetime of free and conjugated fluorescein in various environments," *Journal of Polymer Science: Polymer Letters Edition* **18**, 815–822 (12 1980).